# GROUND MOVING TARGET IMAGING BY SYNTHETIC APERTURE RADAR BASED ON AN UNIFIED FRAMEWORK OF KEYSTONE TRANSFORMATION

*Lei Yang, Lifan Zhao, Lu Wang, Guoan Bi*

School of Electrical and Electronic Engineering, Nanyang Technological University, Singapore
{yanglei, zhao0145, wa0001lu, egbi}@ntu.edu.sg

## ABSTRACT

This paper presents a new SAR ground moving target imaging (GMTIm) algorithm based on an unified framework of Keystone transformation (KT). To combat the inherent range-azimuth coupling, an tandem two-step strategy is designed, where the range decoupling is implemented by polar format algorithm (PFA) and the azimuth decoupling is finished by an novel time-frequency representation method that is Lv's distribution (LVD). We show, mathematically, that the azimuth resampling of PFA has inherently the same mechanism as the KT, and also, the LVD achieves the optimal performance when it is performed in accordance with the KT principle. Therefore, multiple moving targets can be imaged simultaneously. Focused targets' responses can be obtained in both range and azimuth dimensions. Isotropic point target simulation is designed, and experiments are carried out to validate our proposed SAR-GMTIm algorithm.

***Index Terms***— Synthetic aperture radar (SAR), ground moving target imaging, Keystone transformation, polar format algorithm, Lv's distribution.

## 1. INTRODUCTION

Recently, there has been increasing interests in addressing SAR ground moving target imaging (GMTIm) [1, 2]. In general, target radial velocity will result in displaced response, and along-track velocity and radial acceleration will lead to image defocusing [1]. Multichannel SAR in along-track configuration is preferred in SAR-GMTIm, since it is convenient to suppress the clutter that is known as the echoes from the stationary background scene [3, 4].

Regardless of imaging for stationary scene or moving targets, it can be interpreted as removal of inherent coupling between range and azimuth. For instance, in SAR imaging of stationary scene, various SAR image formation algorithms [5, 6] have been introduced. All these algorithms can be categorized as a process of correcting the range migration that is known as coupling between range frequency and azimuth slow-time. PFA is the most popular one because it is conceptually simple and highly efficient [7, 8]. Since the range walk or linear component of the range migration is believed to be the most significant component in achieving stationary scene image, PFA is introduced to correct the range walk under planar wavefront assumption. In SAR-GMTIm scenario, both the radar and target movements vary the range migration. Due to the lack of a prior knowledge of the target trajectory, it is challenging for fully correcting the range migration [9]. Thanks to the Keystone transformation (KT) [10], it is capable of correcting an arbitrary range walk without the kinetic information about the moving target [9].

This project was sponsored by Temasek Laboratories @ Nanyang Technological University (NTU), Singapore.

However, in SAR-GMTIm, the KT can only achieve a preliminary focusing in range dimension. Due to residual azimuth phase modulation (APM), further azimuth refocusing is required. In this paper, we realize the azimuth refocusing under time-frequency representation (TFR) [11–15], and the novel Lv's distribution (LVD) is employed [11]. We will demonstrate the APM in TF related correlation function is a coupling between Doppler frequency and azimuth slow-time. LVD is adopted to correct the linear coupling. Because both the PFA and LVD can be interpreted in accordance with the KT mechanism for the decoupling in range and azimuth, respectively. A unified framework of KT is proposed for SAR-GMTIm. It is possible to image multiple moving targets, simultaneously, and focused target responses in range and azimuth can be obtained. Simulation results can validate the effectiveness of our proposed algorithm.

## 2. SAR-GMTIm SIGNAL MODEL

In this paper, along-track multichannel SAR is employed for further clutter suppression to enhance signal-to-clutter-noise ratio (SCNR) [3, 4]. Assume the reference channel position is $\mathbf{q}_0(t_n)$ during coherent processing interval (CPI), where $t_n$ is the slow-time variable. Other channels can be generally expressed with the position $\mathbf{q}_i(t_n)$ = $\mathbf{q}_0(t_n) + \mathbf{d}_i$, where $\mathbf{d}_i = d_i\vec{\mathbf{x}}$, $d_i$ is the $i$-th channel separation from the reference and $\vec{\mathbf{x}}$ is the unit vector along the airborne SAR flight track or azimuth direction.

Consider the moving target trajectory

$$\mathbf{r}_t(t_n) = \mathbf{R}_0 + \mathbf{r}_0 + \mathbf{v}_t t_n + \mathbf{a}_t t_n^2 \tag{1}$$

where both the target velocity $\mathbf{v}_t$ and acceleration $\mathbf{a}_t$ are formulated to facilitate maneuvering target imaging, $\mathbf{R}_0$ is the reference range vector from the origin of coordinate system we concerned to the observing scene center, and $\mathbf{r}_0$ is the target location offset from the scene center. The radar-to-target range for the reference and $i$-th channel are

$$|\mathbf{R}_{0t}(t_n)| = |\mathbf{r}_t(t_n) - \mathbf{q}_0(t_n)| \tag{2}$$

$$|\mathbf{R}_{it}(t_n)| = |\mathbf{r}_t(t_n) - \mathbf{q}_i(t_n)| \ , \tag{3}$$

respectively. Assuming radar pulses with bandwidth $B$ about carrier frequency $f_0$ are transmitted, the moving target spectra received by the reference and $i$-th channel are

$$S_{0t}(k, t_n) = \exp(-jk\,|\mathbf{R}_{0t}(t_n)|) \tag{4}$$

$$S_{it}(k, t_n) = \exp(-jk\,|\mathbf{R}_{it}(t_n)|) \ , \tag{5}$$

respectively, where $k = 4\pi(f_0 + \Delta f)/c$ denotes the wavenumber, $\Delta f \in [-B/2, B/2]$ is the transmitting frequency variation, and $c$ is the speed of light.

Since all the SAR channels travel precisely along the same path but delayed in time, we have $\mathbf{q}_i(t_n - d_i/v) = \mathbf{q}_0(t_n)$, where the $i$-th channel is assumed leading the reference and $v$ is the speed of the airborne SAR. Thus, the echoes from the clutter have equivalent contribution for the clutter imaging among all the channels [4]. However, the moving target position will definitely change within the time-delay $d_i/v$. From [4], the moving target radial velocity $v_r$ dominates the difference of radar-to-target range between the $i$-th and reference channel. Therefore, the time-shifted radar-to-target range of the $i$-th channel can be approximately written as

$$|\mathbf{R}_{it}(t_n - d_i/v)| \approx |\mathbf{R}_{0t}(t_n)| - v_r d_i/v \ . \tag{6}$$

Then, the clutter can be simply suppressed by subtracting the spectrum of the reference channel from that of the time-shifted $i$-th channel [4], and the result becomes

$$\begin{aligned} S(k, t_n) &= S_{it}(k, t_n - d_i/v) - S_{0t}(k, t_n) \\ &\approx A \cdot S_{0t}(k, t_n) \exp(j\Phi_{\mathrm{In}}/2) \end{aligned} \tag{7}$$

where $A = 2j\sin(\Phi_{\mathrm{In}}/2)$ denotes the complex amplitude, and $\Phi_{\mathrm{In}} \approx 4\pi v_r d_i/\lambda v$ is the interferometry phase [4]. As noticed in (7), to achieve a focused SAR moving target image, $S_{0t}(k, t_n)$ is to be handled.

## 3. KEYSTONE TRANSFORMATION

To investigate $S_{0t}(k, t_n)$, $|\mathbf{R}_{0t}(t_n)|$ should be expanded into Taylor series with respect to $t_n$ as

$$|\mathbf{R}_{0t}(t_n)| \approx R(0) + \dot{R}(0)t_n + \Psi(t_n) \tag{8}$$

where $R(0) = |\mathbf{R}_{0t}(0)|$, $\dot{R}(0) = \left|\dot{\mathbf{R}}_{0t}(0)\right|$, and $\Psi(t_n)$ is the summation of quadratic and higher order terms. Substituting (8) into the clutter-suppressed spectrum (7), we have

$$S(k, t_n) = \exp[-jk(R(0) + \dot{R}(0)t_n + \Psi(t_n))] \tag{9}$$

where both the amplitude and the constant interferometry phase are dropped for simplicity. As noticed in (9), the wavenumber $k$ is coupled with the slow-time variable $t_n$. This coupling is referred to the range migration, which is known as the inherent problem in achieving a focused SAR image. The KT is introduced by rescaling the slow-time $t_n$ in each sample of $k$ [9, 10]. The KT operator is defined as

$$kt_n = (k_0 + \Delta k)t_n = k_0\tilde{t}_n \tag{10}$$

where $k_0{=}4\pi f_0/c{=}4\pi/\lambda$ is the wavenumber centroid, $\lambda$ is the radar wavelength, $\Delta k{=}4\pi\Delta f/c$ is the wavenumber variation, and $\tilde{t}_n$ is the new slow-time variable to cope with the KT operation (10). After the KT processing, (9) becomes

$$S(k, \tilde{t}_n) = \exp[-j(kR(0) + k_0\dot{R}(0)\tilde{t}_n + k\Psi(\frac{k_0\tilde{t}_n}{k_0 + \Delta k}))] \ . \tag{11}$$

In (11), the coupling is removed at least up to the linear component of $\tilde{t}_n$. When the high order terms, $k\Psi(\cdot)$, are ignorable, the target can be imaged by simply applying Fourier transform (FT) with respect to $k$ and $\tilde{t}_n$, respectively.

## 4. PROPOSED SAR-GMTIm ALGORITHM

However, in practice, the high-order terms should be considered for high-resolution SAR imaging. Therefore, the above-mentioned KT can only achieve a preliminary range-focused target image [9]. For focused target image in both range and azimuth dimensions, in this section, a new SAR-GMTIm algorithm is proposed, which is consisted of range decoupling by PFA and azimtuh decoupling by LVD. Both the steps are shown to be in accordance with the KT mechanism.

### 4.1. Range Decoupling By PFA

Commonly, SAR forms an image in a 2 dimensional (2-D) plane of slant-range and azimuth, and we can specifically define the following vectors as

$$\begin{aligned} &\mathbf{R}_0 = R_0\vec{\mathbf{r}}, \ \ \mathbf{r}_0 = x\vec{\mathbf{x}} + r\vec{\mathbf{r}}, \\ &\mathbf{v}_t = v_x\vec{\mathbf{x}} + v_r\vec{\mathbf{r}}, \ \ \mathbf{a}_t = a_x\vec{\mathbf{x}} + a_r\vec{\mathbf{r}} \end{aligned} \tag{12}$$

where $\vec{\mathbf{r}}$ represents unit vector of slant-range. Suppose the airborne SAR works on broadside mode and with zero squint angle at mid-CPI. Position of the reference channel can be specifically given as $\mathbf{q}_0(t_n) = u_n\vec{\mathbf{x}} = vt_n\vec{\mathbf{x}}$.

In the PFA, planar wavefront assumption and far-field hypothesis are employed [7]. Therefore, by assuming the reference $|\mathbf{R}_0 - \mathbf{q}_0(t_n)|$ is much larger than the extent of observing scene, it is feasible and reasonable to approximate $|\mathbf{R}_{0t}(t_n)|$ up to the second order of $\tilde{t}_n$. Then, (7) becomes

$$\begin{aligned} S(k, t_n) \approx \exp[-jk(&\sqrt{R_0^2 + u_n^2} + \frac{R_0 r - u_n x}{\sqrt{R_0^2 + u_n^2}} \\ &+ \frac{(R_0 + r)v_r - u_n v_x}{\sqrt{R_0^2 + u_n^2}}t_n \\ &+ \frac{1}{2}(\frac{v_x^2 + v_r^2}{\sqrt{R_0^2 + u_n^2}} + \frac{(R_0 + r)a_r}{\sqrt{R_0^2 + u_n^2}})t_n^2)] \ . \end{aligned} \tag{13}$$

In the PFA, (13) in polar format $(k, t_n)$ is required to be resampled into rectangle format $(k_r, k_x)$ by using the two sequential interpolators $k_r{=}kR_0/\sqrt{R_0^2 + u_n^2}$ and $k_x{=}{-}k_r u_n/R_0$. Then, we obtain

$$\begin{aligned} S(k_r, k_x) \approx \exp[&-j(k_r r + k_x x + k_x v_x t_n \\ &+ k_r\frac{(R_0 + r)v_r}{R_0}t_n + k_r(\frac{v_x^2 + v_r^2}{2R_0} + \frac{(R_0 + r)a_r}{2R_0})t_n^2)] \ . \end{aligned} \tag{14}$$

To further simplify (14), some latent relations are to be exploited. Firstly, we have $k_x{=}{-}k_r u_n/R_0$ that is the azimuth interpolator, where $u_n$ is the azimuth sample position before the PFA processing. It can be noticed that the azimuth wavenumber $k_x$ is not linearly related with $u_n$ but has dependence on the range wavenumber $k_r$. To remove this dependence, during the azimuth resampling, an new position $\tilde{u}_n$ is introduced to represent a uniform azimuth sample positions along all the samples of $k_r$. By referring to the azimuth samples at $k_r{=}k_0$, we have $k_x{=}{-}k_0\tilde{u}_n/R_0$. Further, it can be found that $k_r u_n{=}k_0\tilde{u}_n$, $k_r t_n{=}k_0\tilde{t}_n$ and $\tilde{u}_n{=}v\tilde{t}_n$. At this point, (14) can be further simplified as

$$\begin{aligned} S(k_r, k_x) \approx \exp[&-j(k_r r + k_x x + k_0\frac{(R_0 + r)v_r}{R_0}\tilde{t}_n \\ &+ k_0(\frac{(v - v_x)^2 + v_r^2}{2R_0} - \frac{v^2}{2R_0} + \frac{(R_0 + r)a_r}{2R_0})\tilde{t}_n^2)] \ . \end{aligned} \tag{15}$$

By further analyzing the PFA, it can be found that the azimuth interpolator $k_r t_n$=$k_0 \tilde{t}_n$ is actually in accordance with the KT mechanism (10), where $k_r$ is the range wavenumber after the range resampling in the PFA. Therefore, the range walk of stationary scene and moving targets can be removed simultaneously by the PFA. This can avoid separate processing steps for stationary scene and moving target, respectively. Furthermore, from (15), range focusing can be achieved by simply applying FT in terms of $k_r$. For further azimuth focusing, residual APM should be handled.

### 4.2. Azimuth Decoupling By LVD

By substituting $k_x = -k_0 v\tilde{t}_n/R_0$ into (15), we can express the azimuth signal only with respect to $\tilde{t}_n$ as

$$s(\tilde{t}_n) = \exp[j2\pi f_d \tilde{t}_n + j\pi\gamma_d \tilde{t}_n^2] \tag{16}$$

where (16) is formulated into a LFM form with Doppler centroid frequency $f_d$=$f_{dc} - f_{dt}$ and chirp rate $\gamma_d = \gamma_{dc} - \gamma_{dt}$, and

$$\begin{aligned} f_{dc} &= \frac{2v}{\lambda}\frac{x}{R_0},\ f_{dt} = \frac{2v}{\lambda}\frac{(R_0+r)v_r}{R_0},\ \gamma_{dc} = \frac{2}{\lambda}\frac{v^2}{R_0}, \\ \gamma_{dt} &= \frac{2}{\lambda}\left(\frac{(v-v_x)^2+v_r^2}{R_0} + \frac{(R_0+r)a_r}{R_0}\right). \end{aligned} \tag{17}$$

To incorporate multiple moving targets, (16) becomes a multi-component LFM model as

$$s(\tilde{t}_n) = \sum_{k=1}^{K} \exp[j2\pi f_d^k \tilde{t}_n + j\pi\gamma_d^k \tilde{t}_n^2] \tag{18}$$

where each moving target signature is characterized by one LFM component with the linear and quadratic parameters $f_d^k$=$f_{dc}^k - f_{dt}^k$ and $\gamma_d^k$=$\gamma_{dc} - \gamma_{dt}^k$, respectively.

In this paper, LVD [11] is adopted to represent the multiple moving targets. To compute an LVD representation, a parametric symmetric instantaneous autocorrelation function (PSIAF) [11] is defined and calculated as

$$\begin{aligned} R_s^C(\tau,\tilde{t}_n) &= s(\tilde{t}_n + \frac{\tau+a}{2}) s^*(\tilde{t}_n - \frac{\tau+a}{2}) \\ &= \sum_{k=1}^{K} \exp[j2\pi f_d^k(\tau+a) + j2\pi\gamma_d^k(\tau+a)\tilde{t}_n] \\ &\quad + \sum_{k=1}^{K-1}\sum_{l=k+1}^{K} R_{s_{kl}}^C(\tau,\tilde{t}_n) + R_{s_{lk}}^C(\tau,\tilde{t}_n) \end{aligned} \tag{19}$$

where the superscript * denotes the conjugate operator, $\tau$ is the time-lag variable, $a$ is a constant time-delay parameter, and $R_{s_{kl}}^C(\cdot)$ denotes one of cross-terms of the PSIAF. As noticed in (19), the time-lag variable $\tau$ is coupled with the PFA interpolated slow-time variable $\tilde{t}_n$. This is the inherent mechanism causing the degradation in TFR. Furthermore, this coupling can be interpreted as the migration of Doppler frequency $\gamma_d^k(\tau+a)$ across the slow-time $\tilde{t}_n$. To remove this linear Doppler migration, a scaling process in LVD is introduced as

$$\Gamma[R_s^C(\tau,\tilde{t}_n)] = R_s^C(\tau, \frac{\tilde{\tilde{t}}_n}{(\tau+a)h}) \tag{20}$$

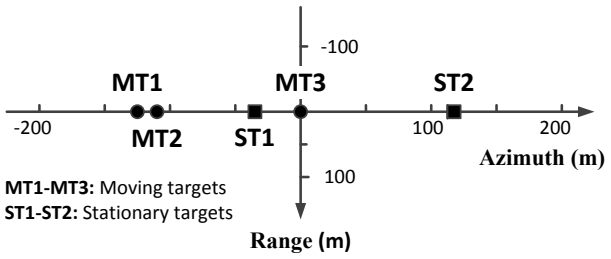


**Fig. 1**. Moving target ground truth.

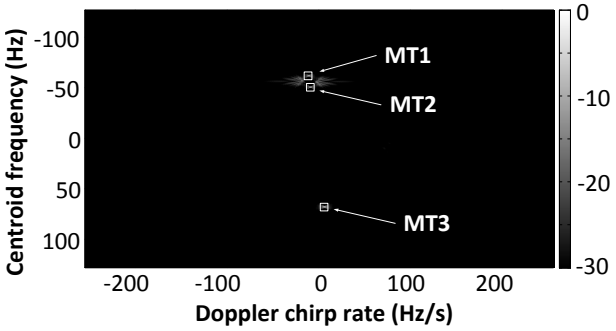


**Fig. 2**. Moving target representation by LVD.

where $\tilde{\tilde{t}}_n$ is the scaled slow-time and $h$ is the scaling factor. Then, the LVD representation can be obtained as

$$\begin{aligned} \mathcal{L}_s(\hat{f}_d,\hat{\gamma}_d) &= \mathcal{F}_{\tilde{\tilde{t}}_n}\left\{\mathcal{F}_\tau\left\{\Gamma[R_s^C(\tau,\tilde{t}_n)]\right\}\right\} \\ &= \sum_{k=1}^{K}\mathcal{L}_{s_k}(\hat{f}_d,\hat{\gamma}_d) + \sum_{k=1}^{K-1}\sum_{l=k+1}^{K}\mathcal{L}_{s_{kl}}(\hat{f}_d,\hat{\gamma}_d) \end{aligned} \tag{21}$$

where $\mathcal{F}_\tau$ and $\mathcal{F}_{\tilde{\tilde{t}}_n}$ are the FT operators with respect to $\tau$ and $\tilde{\tilde{t}}_n$, respectively. In (21), $\mathcal{L}_{s_{kl}}(\cdot)$ is one of the cross-terms of the LVD representation. As it has been concluded in [11], the LVD maintains asymptotic linearity, and the cross-terms have ignorable amplitude compared with that of auto-terms when the CPI is properly selected large enough. According to [11], the two parameters, $a$ and $h$, are both required to be one for the optimal performance of LVD. In such a case, the LVD representation modulus can be given as

$$\left|\mathcal{L}_s(\hat{f}_d,\hat{\gamma}_d)\right| = \sum_{k=1}^{K}\delta(\hat{f}_d - f_d^k)\delta(\hat{\gamma}_d - \gamma_d^k) \tag{22}$$

where $\delta(\cdot)$ is Dirac delta function representing the LVD spread function along the axis $\hat{f}_d$ and $\hat{\gamma}_d$.

Focusing on the LVD implementation, the most significant step is the scaling operation as shown in (20). By further observing (20), when $a$ and $h$ are both set to one, the scaling process can be specifically written as $(1+\tau)\tilde{t}_n$=$\tilde{\tilde{t}}_n$. Obviously, it is in accordance with the KT mechanism (10). Therefore, in achieving azimuth focused target image, LVD is adopted for removing the linear Doppler coupling.

### 4.3. SAR-GMTIm Algorithm

From the LVD representation in (22), each moving target is represented as a distinct peak on the Doppler centroid frequency and chirp

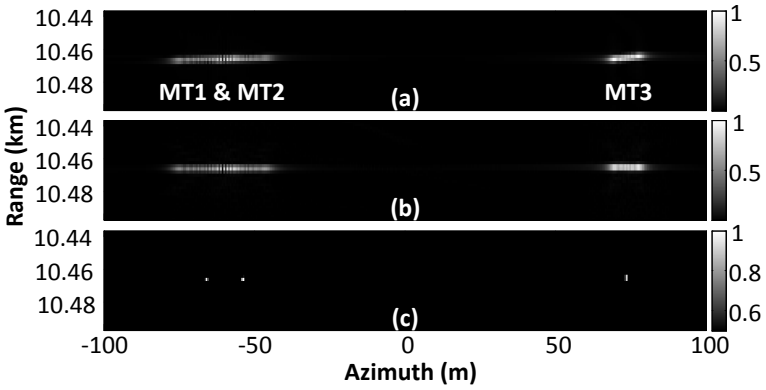


**Fig. 3**. SAR-GMTIm results by (a) directly FT, (b) PFA and (c) proposed algorithm, respectively.

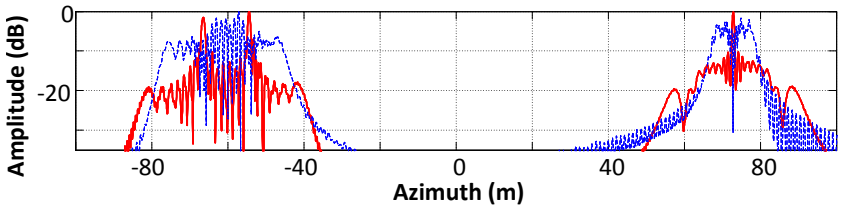


**Fig. 4**. Azimuth responses of Fig. 3(b) (dashed line) and Fig. 3(c) (solid line).

rate (CFCR) domain $(\hat{f}_d, \hat{\gamma}_d)$. The Doppler parameters, $f_d^k$ and $\gamma_d^k$, for each moving target can be obtained by directly reading the peak' coordinates in the CFCR domain.

The Doppler centroid frequency, $f_d^k$, can be used for estimation of the target radial velocity $v_r^k$ and further target geo-location. The Doppler chirp rate, $\gamma_d^k$, can be utilized for estimation of the target along-track velocity $v_a^k$ and radial acceleration $a_r^k$, and simultaneously, the target defocusing can be removed by matched-filtering. Since multiple moving targets can be represented by LVD, all the targets can be refocused simultaneously under the representation.

## 5. EXPERIMENTS

To validate the proposed algorithm, point target simulation is carried out. In the simulation, an airborne SAR is designed. The SAR is supposed to be an X-band radar with carrier frequency of 9.75GHz, bandwidth of 75MHz, and PRF of 1000Hz. Tri-channel SAR system is considered, where the spacing between the two adjacent channels is 0.2m. The airborne SAR is assumed flying with a constant velocity 150m/s and the nearest range to the observing scene center 10km. The CPI for moving target imaging is approximately 2s. The moving target is simulated as the ground truth given in Fig. 1, where both the velocity and acceleration of the moving targets are randomly selected. In addition, two stationary targets are simulated for representing the clutter.

According to our proposed algorithm, after PFA [7] image formation and multichannel clutter suppression [4], LVD is used to represent the multiple moving targets. The LVD representation for MT1-MT3 can be found in Fig. 2, where each moving target is represented as a distinct peak and indicated with respect to the target ID. By reading all the targets representative Doppler chirp rates, the multiple moving targets can be refocused in Fig. 3(c).

Additionally, in Fig. 3, we demonstrate the SAR-GMTIm results by directly FT and PFA as shown in Fig. 3(a) and (b), respectively. As noticed in Fig. 3(a), due to uncorrected range walk, the moving targets are defocused in both range and azimuth dimensions. The range defocusing is obvious for MT3. Besides, as MT1 and MT2 are closely located, their responses are defocused and overlapped with each other. Using the PFA, the range walk is corrected under the KT mechanism. The range defocusing is removed as shown in Fig. 3(b), though azimuth defocusing still exist due to high order APM. As seen in Fig. 3(c), the azimuth defocusing is further removed under the LVD representation that is in accordance with the KT. In Fig. 4, the azimuth responses of Fig. 3(b) and (c) are shown as the dashed and solid lines, respectively. From the comparison, the refocusing performance by our proposed algorithm can be found.

## 6. CONCLUSION

This paper proposes a new SAR-GMTIm algorithm based on an unified framework of KT. The algorithm consists of two steps that are PFA for range decoupling and LVD for azimuth decoupling. As we have demonstrated mathematically, both the implementations of range and azimuth decoupling are in accordance with the KT mechanism. Therefore, multiple moving targets can be imaged, simultaneously. Focused target responses in both range and azimuth can be obtained. Simulation results have validated our proposed algorithm.

## 7. REFERENCES


[1] Jen King Jao and Ali Yegulalp, "Multichannel synthetic aperture radar signatures and imaging of a moving target," *Inverse Problems*, vol. 29, no. 5, pp. 054009, 2013.

[2] Guangcai Sun, Mengdao Xing, Xiang-Gen Xia, Yirong Wu, and Zheng Bao, "Robust ground moving-target imaging using derampkeystone processing," *Geoscience and Remote Sensing, IEEE Transactions on*, vol. 51, no. 2, pp. 966–982, Feb 2013.

[3] H.S.C. Wang, "Mainlobe clutter cancellation by dpca for space-based radars," in *Aerospace Applications Conference, 1991. Digest., 1991 IEEE*, Feb 1991, pp. 1/1–128.

[4] Ross W. Deming, "Along-track interferometry for simultaneous sar and gmti: application to gotcha challenge data," 2011.

[5] Walter G Carrara, Ron S Goodman, and Ronald M Majewski, "Spotlight synthetic aperture radar- signal processing algorithms(book)," *Norwood, MA: Artech House, 1995.*, 1995.

[6] R. Solimene, I. Catapano, G. Gennarelli, A. Cuccaro, A. Dell'Aversano, and F. Soldovieri, "Sar imaging algorithms and some unconventional applications: A unified mathematical overview," *Signal Processing Magazine, IEEE*, vol. 31, no. 4, pp. 90–98, July 2014.

[7] Ross Deming, Matthew Best, and Sean Farrell, "Polar format algorithm for sar imaging with matlab," 2014.

[8] Daiyin Zhu and Zhaoda Zhu, "Range resampling in the polar format algorithm for spotlight sar image formation using the chirp z -transform," *Signal Processing, IEEE Transactions on*, vol. 55, no. 3, pp. 1011–1023, March 2007.

[9] Daiyin Zhu, Yong Li, and Zhaoda Zhu, "A keystone transform without interpolation for sar ground moving-target imaging," *Geoscience and Remote Sensing Letters, IEEE*, vol. 4, no. 1, pp. 18–22, Jan 2007.

[10] R.P. Perry, R.C. DiPietro, and R. Fante, "Sar imaging of moving targets," *Aerospace and Electronic Systems, IEEE Transactions on*, vol. 35, no. 1, pp. 188–200, Jan 1999.

[11] Xiaolei Lv, Guoan Bi, C. Wan, and Mengdao Xing, "Lv's distribution: Principle, implementation, properties, and performance," *Signal Processing, IEEE Transactions on*, vol. 59, no. 8, Aug 2011.

[12] Yu Ding and Jr. Munson, D.C., "Time-frequency methods in sar imaging of moving targets," in *Acoustics, Speech, and Signal Processing (ICASSP), 2002 IEEE International Conference on*, May 2002, vol. 3, pp. III–2881–III–2884.

[13] S. Barbarossa, P. Di Lorenzo, P. Vecchiarelli, A. Silvi, and A. Bruner, "Parameter estimation of 2d polynomial phase signals: An application to moving target imaging with sar," in *Acoustics, Speech and Signal Processing (ICASSP), 2013 IEEE International Conference on*, May 2013, pp. 4554–4558.

[14] J.C. Wood and D.T. Barry, "Radon transformation of time-frequency distributions for analysis of multicomponent signals," *Signal Processing, IEEE Transactions on*, vol. 42, no. 11, pp. 3166–3177, Nov 1994.

[15] L.B. Almeida, "The fractional fourier transform and time-frequency representations," *Signal Processing, IEEE Transactions on*, vol. 42, no. 11, pp. 3084–3091, Nov 1994.